Mechanism for Collective Energy Transfer from Neutral Beam-Injected Ions to Fusion-Born Alpha Particles on Cyclotron Timescales in a Plasma

R. O. Dendy,[1,2] B. Chapman-Oplopoiou,[1] B. C. G. Reman,[2] and J. W. S. Cook[1]
[1]*UKAEA-CCFE, Culham Science Centre, Abingdon OX14 3DB, United Kingdom*
[2]*Centre for Fusion, Space and Astrophysics, Department of Physics, Warwick University, Coventry CV4 7AL, United Kingdom*

(Received 15 February 2022; revised 19 December 2022; accepted 8 February 2023; published 10 March 2023)

Helium ash alpha particles at ∼100 keV in magnetically confined fusion plasmas may have the same Larmor radius, as well as cyclotron frequency, as the energetic beam-injected deuterons that heat the plasma. While the velocity-space distribution of the helium ash is monotonically decreasing, that of the energetic deuterons is a delta function in the edge plasma. Here we identify, by means of first principles particle-in-cell computations, a new physical process by which Larmor radius matching enables collective gyroresonant energy transfer between these two colocated minority energetic ion populations, embedded in majority thermal plasma. This newly identified nonlinear phenomenon rests on similar underlying physics to widely observed ion cyclotron emission from suprathermal minority ion populations.

DOI: 10.1103/PhysRevLett.130.105102

Future magnetically confined fusion (MCF) plasmas will be sustained at high temperatures > 20 keV by collisional heating from alpha particles born at 3.5 MeV in reactions between thermal deuterons and tritons. The lifetime of these plasmas will greatly exceed the slowing-down time of alpha particles, whose thermalizing distribution in velocity space will approximate to a monotonically decreasing Lorentzian [1], with characteristic energy of order a few hundred keV. The cool core (< 100 keV) of this minority population, comprising alpha particles which have given up most of their birth energy, is referred to as "helium ash." The negative slope of the velocity-space distribution implies that electromagnetic waves that enter into wave-particle resonance with the thermalizing alpha particles may be damped.

A second minority suprathermal ion population is typically created by neutral beam injection (NBI) at energies ∼100 keV, whose primary purpose is usually to heat the thermal ions in the MCF plasma core. Recent studies [2–4] show that collective relaxation of a freshly ionized subset of the NBI ions, with an initially delta-function velocity distribution in the edge plasma near the injection point, excites the radiation in the ion cyclotron range of frequencies that is observed in the KSTAR tokamak [2] and LHD heliotron stellarator [3,4]. This is a form of ion cyclotron emission (ICE), whose power spectrum typically exhibits several strongly suprathermal peaks at low integer harmonics of the cyclotron frequency of the injected ions. ICE is widely observed from MCF plasmas. In addition to historical observations from the TFR [5] and JET [6,7] tokamaks, and from deuterium-tritium plasmas in JET [8,9] and TFTR [10], ICE has recently been reported and analyzed from the KSTAR [2,11–13], JT-60U [14,15], DIII-D [16,17], ASDEX-Upgrade [18–21], TUMAN-3M [22,23], NSTX-U [24,25] and EAST [26] and JET [27] tokamaks, and from LHD [3,4,28–30]. ICE is under consideration as a fast-ion diagnostic for ITER [31–33]; it is also observed from solar-terrestrial plasmas [34–38], and may be present downstream of supernova remnant shocks [39].

ICE is driven by the magnetoacoustic cyclotron instability (MCI) [2,4,8–13,17–21,34–36,39–54], which arises when a strongly non-Maxwellian minority energetic ion population enters cyclotron resonance with a fast Alfvén wave propagating nearly perpendicular to the local magnetic field. This resonance can either be wave-wave [41–43], between cyclotron harmonic waves supported by the minority ions and fast Alfvén waves supported by the bulk plasma, or wave-particle [45,46], at Doppler-shifted cyclotron resonance between the minority ions and the Alfvén wave. To strongly excite the MCI, the local distribution of ions in velocity-space must have a positive gradient with respect to the velocity component perpendicular to the magnetic field, $v_\perp$, in the region of velocity space where $v_\perp \sim v_A$, where v_A is the local value of the Alfvén velocity [4,41,42,45,46].

Particularly relevant to the present study is the observed ICE that is driven by collective relaxation of NBI ions under the MCI, which has been simulated [2–4,17] from first principles using particle-in-cell (PIC)-based kinetic codes, notably EPOCH [55]. These self-consistently solve Maxwell's equations for the electric and magnetic fields $\vec{E}$, $\vec{B}$ and the aggregated particle quantities charge density ρ and current $\vec{J}$, in combination with a fully kinetic treatment of the dynamics of tens or hundreds of millions of computational charged particles which all move and interact self-consistently under the Lorentz force equation. Importantly, this first-principles approach to plasma simulation retains

fully resolved gyro-orbit dynamics, thus capturing the full physics of cyclotron resonant interactions between particles and fields. In both analytical and computational studies, the initial velocity-space distribution of the ICE-relevant NBI ions is approximated by a ring-beam delta function, $f(v_\parallel, v_\perp) \propto \delta(v_\parallel)\delta(v_\perp - u_\perp)$, with argument $u_\perp \sim v_{\mathrm{NBI}}$, where v_{NBI} corresponds to their injection energy. The thermal majority and energetic NBI ions are often of the same species. For example, the NBI ions are sub-Alfvénic deuterons at 80 to 100 keV in KSTAR deuterium plasmas [2], super-Alfvénic and sub-Alfvénic protons at 40 keV in LHD hydrogen plasmas [3], and sub-Alfvénic deuterons at 70 keV in LHD deuterium plasmas [4,30].

In the edge region of a deuterium-tritium MCF plasma undergoing nuclear burning there may therefore coexist two energetic minority ion populations—thermalizing alpha particles, and freshly ionized NBI ions—in addition to the thermal majority ions. The constituent ions in these two minority populations will have comparable cyclotron frequencies and Larmor radii. For example, at the same location in space, there may exist an NBI deuteron and a Helium ash alpha particle which gyrate about the local magnetic field line with the same frequency and Larmor radius. The velocity-space distributions from which these two ions are drawn will be radically different: a monotonic decrease for the alpha particles, implying damping of waves at cyclotron resonance; and an MCI-driving delta function for the NBI ions. These considerations point to an intriguing and potentially important new nonlinear plasma physics phenomenon, which has not been previously identified, to our knowledge.

We report here a new collective process that can rapidly and directly transfer kinetic energy from NBI deuterons to helium ash alpha particles, on cyclotron timescales. Our PIC studies show that the physics involves a generalization of the MCI. The energy transfer between the two energetic ion populations is mediated by the electric and magnetic fields that are collectively excited by the NBI deuterons, and supported also by the bulk thermal plasma. This process dominates the energy flow of the MCI, in contrast to the related ICE case, where the energy flow is dominated by electromagnetic field excitation on the fast Alfvén-cyclotron harmonic wave branch. Under edge plasma conditions, where the velocity-space distribution of the NBI ions approximates to a ring beam, this new effect is found to be strongest for a characteristic helium ash temperature 0.1 MeV which is comparable to the injection energy of the NBI deuterons. The two energetic ion populations have the same cyclotron frequency, and we find that energy transfer occurs predominantly between deuterons and alpha particles that have similar Larmor radii, and involves bunching in gyrophase. To our knowledge, this is the first study of direct local collective energy transfer from NBI ions to alpha particles, on cyclotron timescales, in MCF plasmas. In the demonstration-of-principle simulations reported here, of order 10% of the energy of NBI ions that become ionized in the edge region can be transferred to the alpha particles. Unexplained local excursions in the energy distribution among ion species would be unacceptable in a burning plasma or regulated fusion power plant, and indeed for ITER with its planned 33 MW of NBI used for heating and current drive [56].

We have run PIC calculations of the Maxwell-Lorentz dynamics of tens of millions of interacting particles, together with their self-consistent electric and magnetic fields, drawn from four populations. Two are thermal: the electrons, and the majority deuterons, with $T_D = 5$ keV $= T_e$. Two are energetic minorities. First, the minority NBI deuterons with injection energies $E_{\mathrm{NBI}} = 80$, 140, or 200 keV, which are represented by an initial delta function in perpendicular velocity. Second, the minority alpha particles, which are represented by a Maxwellian with temperatures $T_{\mathrm{th},\alpha} = 0.1$, 0.5, or 1.0 MeV; the lowest of these temperatures is a good approximate model for fully slowed-down helium ash. Simulation parameters are broadly representative of JET plasmas, with electron number density $n_e = 9.8 \times 10^{19}$ m^{-3} and magnetic field strength $B_z = 2.7$ T oriented perpendicular to the 1D3V PIC code spatial domain. It follows that the ratio of NBI ion speed v_{NBI} to local Alfvén speed V_A for the three injection energies is $v_{\mathrm{NBI}}/V_A = 0.66$, 0.87, and 1.04, respectively; for alpha particles at their thermal energy for the three temperatures, the corresponding speed ratio is $v_{\mathrm{Th},\alpha}/V_A = 0.52$, 1.16, and 1.64. The ratios v_{NBI}/V_A and $v_{\mathrm{Th},\alpha}/V_A$ are the key dimensionless parameters governing the physics of the MCI for this model in this regime, and the nine cases examined in Figs. 1 and 2 together cover a range of possible values for the fixed local equilibrium density and magnetic field strength. Each PIC simulation uses 10 150 grid cells with 1000 particles per cell and conserves energy to ~1%. In most cases, the ratio of alpha particles to thermal deuterons $\xi_\alpha = 10^{-3}$, and the ratio of NBI deuterons to thermal deuterons $\xi_{\mathrm{NBI}} = 10^{-3}$. Insofar as these values may be unphysically high, this is necessary to enable the physics to unfold in our PIC simulations using acceptable computational resources. Precedents from previous ICE studies [50,52,53] suggest that the phenomenology is scalable with respect to the concentration of energetic ions.

The multispecies plasma, initialized as above, relaxes, and the time evolution of particle and field energy densities is shown in Fig. 1 for nine representative cases. The right-hand column of Fig. 1 shows baseline ICE-type phenomenology for the relaxation of NBI ions under the MCI, as seen in, for example, Fig. 4 of Ref. [2] and of Ref. [3]. This is dominated by energy transfer from the NBI deuterons to the excited fast Alfvén waves, whereas energy transfer involving the alpha particles is relatively insignificant. The Alfvén waves incorporate the kinetic energy of coherent oscillations of the thermal deuterons, in addition to electric and magnetic fields. Our newly identified effect appears in the left-hand column of Fig. 1: after an initial ICE-type

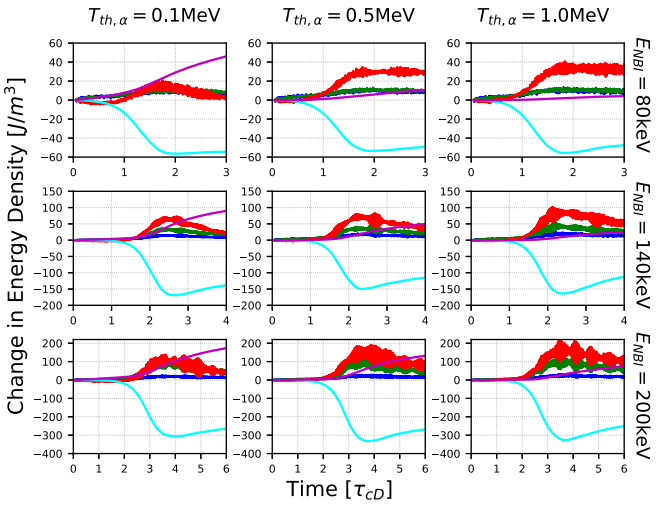

FIG. 1. Time evolution of the change in energy density of particles and electric and magnetic fields in multiple PIC simulations with initial NBI deuteron energies 80, 140, and 200 keV (rows from top to bottom), and initial helium ash temperatures 0.1, 0.5, and 1.0 MeV (columns from left to right). Time is normalized to the deuteron gyroperiod τ_{cD}. The traces, their peaks ordered from top to bottom in the upper left panel, are top (magenta): the change in kinetic energy density of the minority alpha particles; second (red): the change in kinetic energy density of the thermal bulk plasma deuterons; third (green): the energy density of the magnetic field perturbation ΔB_z; fourth (blue): the energy density of the electrostatic field E_x; fifth (cyan): the change in kinetic energy density of the minority energetic NBI deuterons.

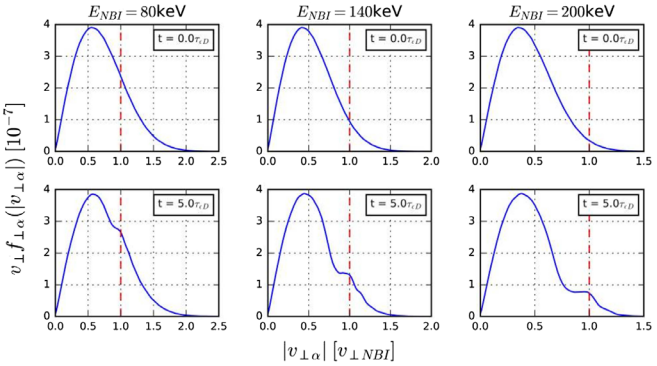

FIG. 2. Perpendicular velocity-space resonance $v_\perp = v_{\perp\mathrm{NBI}}$ with respect to the alpha-particle distributions: Initially at $t = 0$ (upper row); and nonlinearly evolved to $5.0\tau_{cD}$ (lower row). The three columns are for the PIC simulation cases of NBI deuterons, initially distributed as a ring-beam delta-function in perpendicular velocity, with energies 80, 140, and 200 keV. The vertical dashed line (red) denotes where the Larmor radius ($r_L = v_\perp/\Omega_\alpha$) of alpha particles equals that of NBI deuterons. Initially Maxwellian alpha particles with $T_{\mathrm{th},\alpha} = 0.1$ MeV undergo strongly nonlinear interactions resulting in distortions at this resonant velocity. In each panel the alpha-particle velocity is normalized to the NBI deuteron velocity for that case.

phase, in the nonlinear regime the dominant long-term energy transfer is from the minority energetic NBI deuterons to the minority energetic alpha-particle population. About 10% of the total NBI deuteron kinetic energy is lost; the majority of this is transferred to the alpha particles in the cases in the left column of Fig. 1, and these proportions are invariant with respect to ξ_α.

We emphasize that the fully nonlinear treatment presented here is essential to establishing how energy is partitioned between the different ion species in the saturated state. In the Appendix it is established that, conversely, the physics at early times (corresponding to the linear phase) does not provide a guide to the eventual energy partitioning, and in particular the heating of helium ash.

Figure 2 plots snapshots of the distribution in perpendicular velocity space of the alpha particles: initially Maxwellian with $T_{\mathrm{th},\alpha} = 0.1$ MeV at $t = 0$ (upper row); and output from our PIC simulations at $t = 5\tau_{cD}$ (lower row). The three columns are for the cases of NBI deuterons, initially distributed as a ring-beam delta function in perpendicular velocity, with energies 80, 140, and 200 keV. In each panel the alpha-particle velocity is normalized to the NBI deuteron velocity for that case. It is evident from Fig. 2 that the energy flows primarily from the NBI deuterons to alpha particles that have the same perpendicular velocity, causing a distortion around $v_{\perp\alpha} \sim v_{\perp\mathrm{NBI}}$. Recalling that the deuterons and alpha particles have the same cyclotron frequency, it follows that the energy transfer is between ions that have closely similar Larmor radii. This implies that cyclotron resonance is central to the physics of the newly identified energy transfer process.

Gyrobunching in velocity space is therefore expected, and is evident in Fig. 3. This is a snapshot at $t = 2\tau_{cD}$ of the distribution of NBI deuterons with respect to the spatial domain x and gyroangle ϕ, for the 1D3V PIC simulation

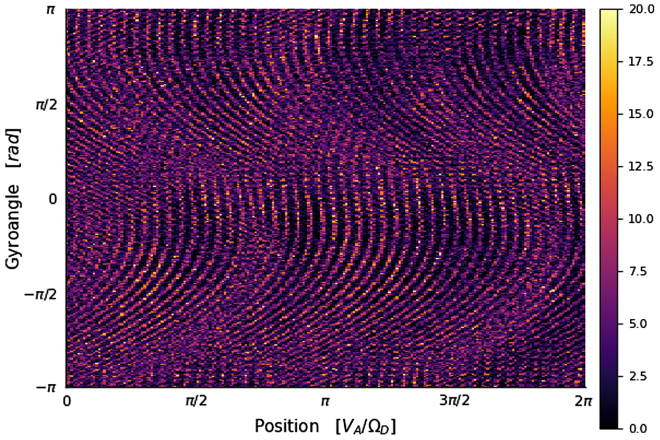

FIG. 3. Nonlinear gyrobunching: a snapshot at $2\tau_{cD}$ (see also Fig. 6) of the distribution of NBI deuterons, initially at 140 keV, with respect to their spatial position x and gyroangle ϕ. This 1D3V PIC simulation is for a thermal deuterium plasma ($T_D = 5$ keV) which also contains a minority alpha-particle population with temperature $T_{\mathrm{th},\alpha} = 0.1$ MeV. The choice of normalization for position facilitates comparison with Fig. 4, see main text.

considered in the central panel of Fig. 1. The S-shaped striations in Fig. 3 are characteristic of cyclotron resonant ion gyrobunching; see, for example, Fig. 3 of Ref. [57] and Fig. 4 of Ref. [50], and references therein.

In Fig. 3, the x-axis units are constructed by normalizing position to V_A/Ω_D, where Ω_D is the deuteron angular cyclotron frequency. This normalization factor has units of meters per radian, which is the inverse of the units used in Fig. 4 for wave number. The range of the x domain is from zero to 2π meters per radian; this facilitates direct conversion from the number of striations counted in Fig. 3 to wave number as considered in Fig. 4, which plots the spatiotemporal Fourier transform of the excited B_z magnetic field component in our simulation. Visual inspection of Fig. 3 indicates that there are 43 striations in the interval from zero to 2π. This implies a wavelength in these units of $\lambda = 2\pi/43[V_A/\Omega_D]$ and hence a wave number $k = 2\pi/\lambda = 43[\Omega_D/V_A]$. This value can be seen to align with the dominant wave number structure in Fig. 4. This field mediates the interaction between deuterons and alpha particles. It is evident from Fig. 4 that its dominant cyclotron harmonic components lie in the range between thirtieth and fortieth, on the fast Alfvén wave branch that extends approximately diagonally from the origin, deviating from linear at higher frequencies. Quasihorizontal low integer cyclotron harmonic waves are visible, here populated by noise through the fluctuation-dissipation theorem [58]. Their intersection with the fast Alfvén branch is the locus of strong MCI drive in edge ICE scenarios; much higher cyclotron harmonics dominate in the scenario considered here, see also the inset of Fig. 4.

The two panels of Fig. 5 compare the power spectra of fields excited in otherwise identical simulations with different concentrations (one negligible) of minority alpha particles with $T_{\mathrm{th},\alpha} = 0.1$ MeV. These spectra are obtained from PIC-hybrid simulations (that is, with fluidized electrons; see Ref. [2]) for NBI deuterons at 140 keV in a deuterium thermal plasma. Each ion species is represented with 400 particles per cell, and the simulation domain has 1024 cells. The spectra result from Fourier transforming the self-consistent fields that are excited in the simulations, summing over a time interval $10\tau_{cD}$. In both cases, the excited (above noise) field energy is bunched with spectral peaks in the two groups of cyclotron harmonics already identified from the full PIC simulation in Fig. 4, around the

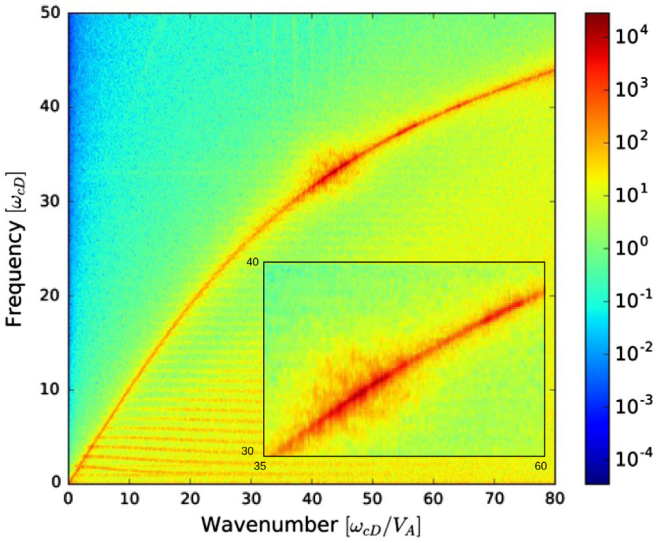

FIG. 4. Spatiotemporal Fourier transform of the excited z component of the magnetic field from the simulation for an NBI deutron energy of 140 keV and $T_{\mathrm{th},\alpha} = 0.1$ MeV. Field energy is concentrated between the thirtieth and fortieth cyclotron harmonics, on and near the fast Alfvén wave branch. The dispersion (manifested as curvature) of the fast Alfvén branch here arises from the first principles Maxwell-Lorentz dynamics of the PIC simulations. Inset: an expanded plot of the region between the 30th and 40th cyclotron harmonics.

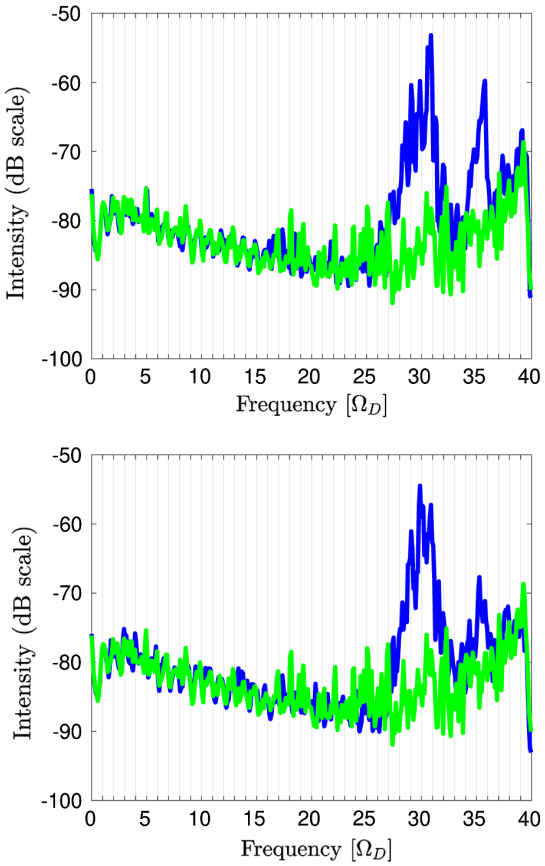

FIG. 5. Frequency power spectra (blue) obtained from the spatiotemporal Fourier transform of excited fields in PIC-based simulations at $t = 10\tau_{cD}$. In both cases NBI deuteron concentration $\xi_{\mathrm{NBI}} = 10^{-3}$. Upper panel: alpha-particle concentration $\xi_\alpha = 10^{-3}$, the scenario of Figs. 1 and 2. Lower panel: negligible $\xi_\alpha = 10^{-6}$, hence a purely NBI-driven ICE scenario. Green traces are the fluctuation-dissipation noise baseline. Frequency is in units of the deuteron (equivalently alpha particle) gyrofrequency. The primary difference between these excited spectra is around the 35th deuteron cyclotron harmonic.

thirtieth and the thirty-fifth. The primary difference is the diminished field energy around the 35th cyclotron harmonic in the upper panel. This reflects energy that has flowed from the NBI deuterons to the alpha particles in the helium ash case of $\xi_\alpha = 10^{-3}$, instead of flowing to the excited fields in the ICE-type case of $\xi_\alpha = 10^{-6}$.

We have identified a new collective cyclotron resonant process that can shift energy rapidly from freshly injected NBI deuterons to thermalizing fusion-born alpha particles, in a majority thermal plasma where both energetic ion species are present. The energy transfer is concentrated between the subset of ions of both species that have similar Larmor radii. The novel process investigated here is accessible only computationally, because of its three-ion-species and intrinsically nonlinear character, and has not previously been considered or identified. For the MCF edge plasma scenario considered here, the selection criterion for the most active subset of ions is effectively governed by the component of the injection energy of the NBI deuterons that is perpendicular to the magnetic field. The physics of energy transfer is a generalization of the MCI, the instability which underlies observations of ICE from MCF plasmas in general and, in particular, from NBI ion populations in the edge plasmas of the KSTAR tokamak and the LHD heliotron-stellarator. This newly identified effect is also likely to be strongest in edge plasmas, where the freshly ionized NBI ions approximate to a ring-beam in velocity space, and energy transfer is to helium ash alpha particles with comparable energies ~0.1 MeV. In the locally uniform demonstration-of-principle simulations presented here, the maximum proportion of NBI deuteron energy lost is of order 10%. It therefore appears possible that noticeable diminution of NBI power delivered to the core plasma could occur by this new process, under conditions where alpha-particle production in fusion reactions is substantial. The present results extend the reach of the MCI in MCF plasma physics, where it has also been identified as a potential mechanism for alpha channeling [59] as well as the driving mechanism for ICE. There may also be consequences, for future investigation, for the confinement and transport of helium ash in the edge plasma. Experimental testing of the present theory could perhaps be carried out using minority energetic Helium ion populations generated, as in Ref. [60], using a three-ion cyclotron resonant heating scenario [61,62]. It is helpful that this approach, like classic minority ion cyclotron resonant heating scenarios (for which see, for example, Fig. 5 of Ref. [63]), predominantly raises the perpendicular energy component of the heated ions, and hence their Larmor radii.

This work received support from the RCUK Energy Programme Grant No. EP/T012250/1. It was carried out within the framework of the EUROfusion Consortium and has received funding from the Euratom research and training programme 2014–2018 and 2019–2020 under Grant Agreement No. 633053. The views and opinions expressed herein do not necessarily reflect those of the European Commission. We acknowledge computational resources and support from the Midlands Plus HPC regional consortium

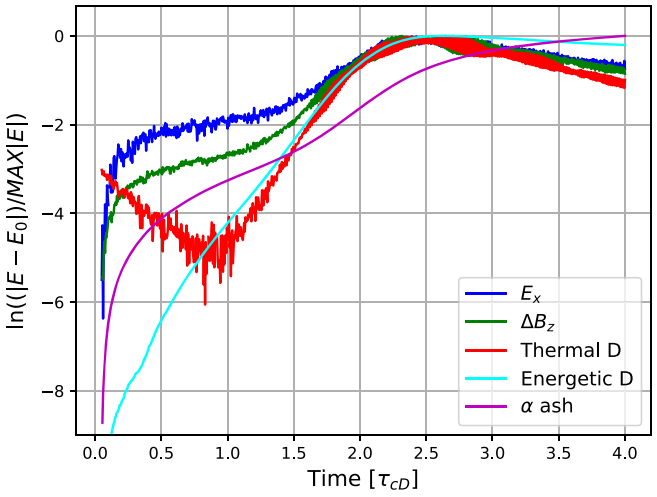

FIG. 6. The scaled natural logarithm of the change, versus time, in the five categories of energy density E plotted in Fig. 1, with identical color coding. The NBI deuteron energy and alpha-particle temperatures are 140 keV and 0.1 MeV, respectively. Here, E_0 and $MAX|E|$ are the initial and maximum absolute values of the plotted component of energy density. The local slope of each trace can be interpreted as an effective instantaneous growth rate.

Appendix: Limitations of a linear-type description.—Figure 6 plots the scaled natural logarithm of the change in the five energy density components against time. For each trace, the local gradient may be interpreted as an effective instantaneous growth rate if the initial transient

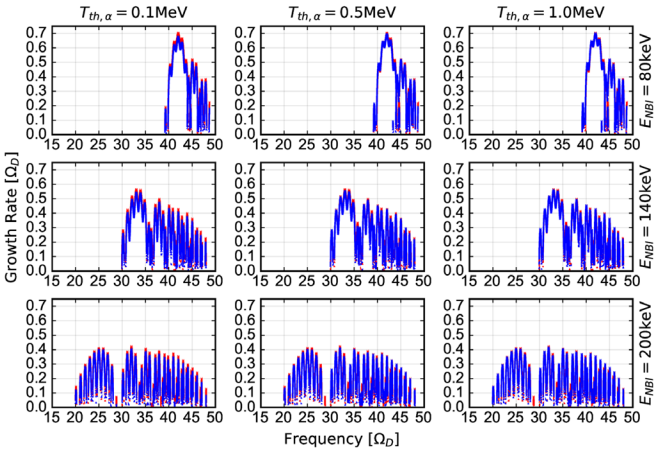

FIG. 7. The linear growth rate of the MCI for the cases shown in Fig. 1 without alpha particles (blue trace) and with the number density ratio ξ_α of alpha particles to deuterons set at 10^{-3} (red trace). Linear growth rates are insensitive (compare columns) to the presence or temperature of alpha particles. They are highly sensitive (compare rows) to the fast Alfvén wave dispersion relation (see also Fig. 4) in the presence of energetic deuterons.

behavior is excluded for $t < 0.2\tau_{cD}$. At early times ($0.2\tau_{cD} \leq t \leq 2\tau_{cD}$) the instantaneous growth rates are not a guide to the partitioning of energy between traces at late time beyond $2\tau_{cD}$, which is dictated by novel emergent nonlinear physics.

Figure 7, which shows at most 2% difference in linear MCI growth rate with (blue trace) and without alpha particles (red trace), further confirms that the linear phase is not a guide to the saturated state and hence, crucially, to the eventual energy partitioning between ion species leading to the heating of helium ash.

[1] D. A. Spong, D. J. Sigmar, K. T. Tsang, J. J. Ramos, D. E. Hastings, and W. A. Cooper, Phys. Scr. **1987**, 18 (1987).
[2] B. Chapman, R. O. Dendy, S. C. Chapman, K. G. McClements, G. S. Yun, S. G. Thatipamula, and M. H. Kim, Nucl. Fusion **59**, 106021 (2019).
[3] B. C. G. Reman, R. O. Dendy, T. Akiyama, S. C. Chapman, J. W. S. Cook, H. Igami, S. Inagaki, K. Saito, and G. S. Yun, Nucl. Fusion **59**, 096013 (2019).
[4] B. C. G. Reman, R. O. Dendy, T. Akiyama, S. C. Chapman, J. W. S. Cook, H. Igami, S. Inagaki, K. Saito, R. Seki, and M. H. Yun, Nucl. Fusion **61**, 066023 (2021).
[5] TFR Equipe Collaboration, Nucl. Fusion **18**, 1271 (1978).
[6] G. A. Cottrell and R. O. Dendy, Phys. Rev. Lett. **60**, 33 (1988).
[7] P. Schild, G. A. Cottrell, and R. O. Dendy, Nucl. Fusion **29**, 834 (1989).
[8] G. A. Cottrell, V. P. Bhatnagar, O. Da Costa, R. O. Dendy, J. Jacquinot, K. G. McClements, D. C. Mccune, M. F. F. Nave, O. Smeulders, and D. F. H. Start, Nucl. Fusion **33**, 1365 (1993).
[9] K. G. McClements, C. Hunt, R. O. Dendy, and G. A. Cottrell, Phys. Rev. Lett. **82**, 2099 (1999).
[10] R. O. Dendy, K. G. McClements, C. N. Lashmore-Davies, G. A. Cottrell, R. Majeski, and S. Cauffman, Nucl. Fusion **35**, 1733 (1995).
[11] S. G. Thatipamula, G. S. Yun, J. Leem, H. K. Park, K. W. Kim, T. Akiyama, and S. G. Lee, Plasma Phys. Control. Fusion **58**, 065003 (2016).
[12] B. Chapman, R. O. Dendy, K. G. McClements, S. C. Chapman, G. S. Yun, S. G. Thatipamula, and M. H. Kim, Nucl. Fusion **57**, 124004 (2017).
[13] B. Chapman, R. O. Dendy, S. C. Chapman, K. G. McClements, G. S. Yun, S. G. Thatipamula, and M. H. Kim, Nucl. Fusion **58**, 096027 (2018).
[14] M. Ichimura, H. Higaki, S. Kakimoto, Y. Yamaguchi, K. Nemoto, M. Katano, M. Ishikawa, S. Moriyama, and T. Suzuki, Nucl. Fusion **48**, 035012 (2008).
[15] S. Sumida, K. Shinohara, M. Ichimura, T. Bando, A. Bierwage, and S. Ide, Nucl. Fusion **61**, 116036 (2021).
[16] K. E. Thome, D. C. Pace, R. I. Pinsker, M. A. Van Zeeland, W. W. Heidbrink, and M. E. Austin, Nucl. Fusion **59**, 086011 (2019).
[17] N. A. Cocker, S. X. Tang, K. E. Thome, J. Lestz, E. Belova, A. Zalzali, R. O. Dendy, W. A. Peebles, K. Barada, R. Hong *et al.*, Nucl. Fusion **62**, 026023 (2022).
[18] R. Ochoukov, R. Bilato, V. Bobkov, B. Chapman, S. C. Chapman, R. O. Dendy, M. Dunne, H. Faugel, M. García-muñoz, B. Geiger *et al.*, Nucl. Fusion **59**, 014001 (2018).
[19] R. Ochoukov, K. G. McClements, R. Bilato, V. Bobkov, B. Chapman, S. C. Chapman, R. O. Dendy, R. M. Dreval, H. Faugel, and J-M. Noterdaeme, Nucl. Fusion **59**, 086032 (2019).
[20] B. Chapman, R. O. Dendy, S. C. Chapman, K. G. McClements, and R. Ochoukov, Plasma Phys. Control. Fusion **62**, 095022 (2020).
[21] L. Liu, R. Ochoukov, K. G. McClements, R. O. Dendy, V. Bobkov, M. Weiland, R. Bilato, H. Faugel, D. Moseev, M. Salewski *et al.*, Nucl. Fusion **61**, 026004 (2020).
[22] L. G. Askinazi, A. A. Belokurov, D. B. Gin, V. A. Kornev, S. V. Lebedev, A. E. Shevelev, A. S. Tukachinsky, and N. A. Zhubr, Nucl. Fusion **58**, 082003 (2018).
[23] L. G. Askinazi, G. I. Abdullina, A. A. Belokurov, V. A. Kornev, S. V. Krikunov, S. V. Lebedev, D. V. Razumenko, A. S. Tukachinsky, and N. A. Zhubr, Tech. Phys. Lett. **47**, 214 (2021).
[24] E. D. Fredrickson, N. N. Gorelenkov, R. Bell, A. Diallo, B. Leblanc, J. Lestz, and M. Podestà, Nucl. Fusion **61**, 086007 (2021).
[25] E. D. Fredrickson, N. N. Gorelenkov, R. E. Bell, A. Diallo, B. P. Leblanc, and M. Podestà, Phys. Plasmas **26**, 032111 (2019).
[26] L. Liu, X. Zhang, Y. Zhu, C. Qin, Y. Zhao, S. Yuan, Y. Mao, M. Li, Y. Chen, and J. Cheng, Rev. Sci. Instrum. **90**, 063504 (2019).
[27] K. G. McClements, A. Brisset, B. Chapman, S. C. Chapman, R. O. Dendy, P. Jacquet, V. Kiptily, M. Mantsinen, B. C. G. Reman, and JET Contributors, Nucl. Fusion **58**, 096020 (2018).
[28] K. Saito, H. Kasahara, T. Seki, R. Kumazawa, T. Mutoh, T. Watanabe, F. Shimpo, G. Nomura, M. Osakabe, M. Ichimura *et al.*, Fusion Eng. Des. **84**, 1676 (2009).
[29] K. Saito, R. Kumazawa, T. Seki, H. Kasahara, G. Nomura, F. Shimpo, H. Igami, M. Isobe, K. Ogawa, and K. Toi *et al.*, Plasma Sci. Technol. **15**, 209 (2013).
[30] B. C. G. Reman, R. O. Dendy, H. Igami, T. Akiyama, M. Salewski, S. C. Chapman, J. W. S. Cook, S. Inagaki, K. Saito, R. Seki, M. Toida, M. H. Kim, S. G. Thatipamula, and G. S. Yu, Plasma Phys. Control. Fusion **64**, 085008 (2022).
[31] K. G. McClements, R. D'inca, R. O. Dendy, L. Carbajal, S. C. Chapman, J. W. S. Cook, R. Harvey, W. W. Heidbrink, and S. D. Pinches, Nucl. Fusion **55**, 043013 (2015).
[32] R. O. Dendy and K. G. McClements, Plasma Phys. Control. Fusion **57**, 044002 (2015).
[33] N. N. Gorelenkov, Plasma Phys. Rep. **42**, 430 (2016).
[34] R. O. Dendy and K. G. McClements, J. Geophys. Res. Space Phys. **98**, 15531 (1993).
[35] K. G. McClements and R. O. Dendy, J. Geophys. Res. Space Phys. **98**, 11689 (1993).
[36] K. G. McClements, R. O. Dendy, and C. N. Lashmore-Davies, J. Geophys. Res. Space Phys. **99**, 23685 (1994).
[37] R. O. Dendy, Plasma Phys. Control. Fusion **36**, B163 (1994).
[38] J. L. Posch, M. J. Engebretson, C. N. Olson, S. A. Thaller, A. W. Breneman, J. R. Wygant, S. A. Boardsen, C. A. Kletzing, C. W. Smith, and G. D. Reeves, J. Geophys. Res. Space Phys. **120**, 6230 (2015).

[39] V. Rekaa, S. C. Chapman, and R. O. Dendy, Astrophys. J. **791**, 26 (2014).
[40] B. Chapman, R. O. Dendy, S. C. Chapman, L. A. Holland, S. W. A. Irvine, and B. C. G. Reman, Plasma Phys. Control. Fusion **62**, 055003 (2020).
[41] V. S. Belikov and Ya. I. Kolesnichenko, Zhurnal Tekhnicheskoi Fiziki **45**, 1798 (1975) [Sov. Phys. Tech. Phys. **20**, 1146 (1976)].
[42] R. O. Dendy, C. N. Lashmore-Davies, and K. Kam, Phys. Fluids B **4**, 3996 (1992).
[43] R. O. Dendy, C. N. Lashmore-Davies, and K. Kam, Phys. Fluids B **5**, 1937 (1993).
[44] R. O. Dendy, K. G. McClements, C. N. Lashmore-Davies, R. Majeski, and S. Cauffman, Phys. Plasmas **1**, 3407 (1994).
[45] R. O. Dendy, C. N. Lashmore-Davies, K. G. McClements, and G. A. Cottrell, Phys. Plasmas **1**, 1918 (1994).
[46] K. G. McClements, R. O. Dendy, C. N. Lashmore-Davies, G. A. Cottrell, S. Cauffman, and R. Majeski, Phys. Plasmas **3**, 543 (1996).
[47] T. Fülöp, Ya. I. Kolesnichenko, M. Lisak, and D. Anderson, Nucl. Fusion **37**, 1281 (1997).
[48] T. Fülöp and M. Lisak, Nucl. Fusion **38**, 761 (1998).
[49] T. Fülöp, N. Lisak, Ya.-I. Kolesnichenko, and D. Anderson, Phys. Plasmas **7**, 1479 (2000).
[50] J. W. S. Cook, R. O. Dendy, and S. C. Chapman, Plasma Phys. Control. Fusion **55**, 065003 (2013).
[51] L. Carbajal and F. Calderón, Phys. Plasmas **28**, 014505 (2021).
[52] L. Carbajal, R. O. Dendy, S. C. Chapman, and J. W. S. Cook, Phys. Plasmas **21**, 012106 (2014).
[53] L. Carbajal, R. O. Dendy, S. C. Chapman, and J. W. S. Cook, Phys. Rev. Lett. **118**, 105001 (2017).
[54] J. W. S. Cook, Plasma Phys. Control. Fusion **64**, 115002 (2022).
[55] T. D. Arber, K. Bennett, C. S. Brady, A. Lawrence-Douglas, M. G. Ramsay, N. J. Sircombe, P. Gillies, R. G. Evans, H. Schmitz, and A. R. Bell, Plasma Phys. Control. Fusion **57**, 113001 (2015).
[56] R. S. Hemsworth, D. Boilson, P. Blatchford, M. Dalla Palma, G. Chitarin, H. P. L. de Esch, F. Geli, N. Dremel, J. Graceffa, D. Marcuzzi, G. Serianni, D. Shah, M. Singh, M. Urbani, and P. Zaccaria, New J. Phys. **19**, 025005 (2017).
[57] J. W. S. Cook, R. O. Dendy, and S. C. Chapman, Plasma Phys. Control. Fusion **53**, 074019 (2011).
[58] R. Kubo, Rep. Prog. Phys. **29**, 255 (1966).
[59] J. W. S. Cook, R. O. Dendy, and S. C. Chapman, Phys. Rev. Lett. **118**, 185001 (2017).
[60] A. Kappatou, M. Weiland, R. Bilato, Ye. O. Kazakov, R. Dux, V. Bobkov, T. Pütterich, and R. M. McDermott, Nucl. Fusion **61**, 036017 (2021).
[61] Y. O. Kazakov, D. van Eester, R. Dumont, and J. Ongena, Nucl. Fusion **55**, 032001 (2015).
[62] J. Faustin, J. Graves, W. Cooper, S. Lanthaler, L. Villard, D. Pfefferlé, J. Geiger, Y. Kazakov, and D. van Eester, Plasma Phys. Control. Fusion **59**, 084001 (2017).
[63] V. P. Bhatnagar, J. Jacquinot, D. F. H. Start, and B. J. T. Tubbing, Nucl. Fusion **33**, 83 (1993).